ENERGY COMPRESSION EXPERIMENTS: SIMULATION OF SMALL-SIZE MCG TO OBTAIN A RADIO FREQUENCY SOURCE

Mladen M. Kekez, High-Energy Frequency Tesla Inc., (HEFTI), 1200 Montreal Road, Building M-51, Ottawa, ON, Canada, K1A 0R6, mkekez@magma.ca

ABSTRACT

The electrically driven system was used to simulate the operation of sub-micro-size MCG. Initially, the maximum voltage at the output of the coil is = 6 kV, and the maximum current through the helical coil is < 4 kA. By compressing the energy stored in the coil, the electromagnetic induction voltage reaches up to 700 kV and the induced current is up to 10 kA. The goal of the work is to convert the available gigawatt power pulse into radio frequency (RF) radiations.

INTRODUCTION

According to the definition given by Novac and Smith[1], the micro-size MCG's are capable of producing the current of up to 13 kA and the maximum voltages of up to 15 kV, with the load of 100 nH and the effective explosive charge of about 10 g. The experimental work by Freeman *et al.*[2] shows that the armature diameters of such helical MCG's are in the range from 0.95 cm to 2.54 cm. Useful data on the small-size MCG are given amongst others also by Chernyshev[3], Fortov *et al.*[4], Kristiansen *et al.*[5], and Selemir *et al.*[6].

In this work the electrically driven system was employed to simulate the operation of sub-micro-size MCG to work as the radio frequency generator. The goal of the work is to convert the available gigawatt power pulse into RF radiations through the use of an oscillatory circuit operating in air.

OSCILLATORY CIRCUIT

In Fig. 1, six-stage Marx generator is represented by the capacitor C_1 (= 7.5 nF) charged to potential V and the closing switch, U_1. Kekez[7] gives the characteristics of this generator.

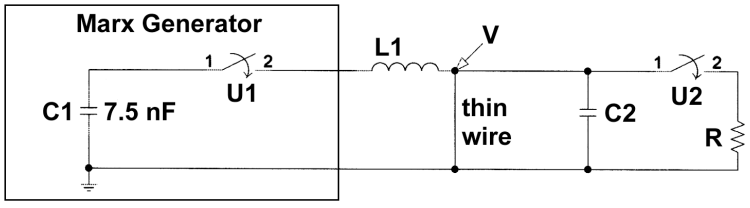

Figure 1. Equivalent circuit of the experimental set-up.

When the switch U_1 is closed and the switch U_2 remains open, the Marx generator of the internal inductance, L_M (= 2.4 μH) is discharged via the coil of the inductance, L_1 (= 9.6 μH) and the thin wire of the inductance L_2 (= 0.6 μH). The current is of oscillatory form because the resistance of the coil, R_C (= 0.1 O) and the resistance of the thin wire R_W (= 2.4 O at T = 300 K) are of small values in regards to other circuit parameters; i.e. $R_C + R_W << \sqrt{(L_1 + L_2 + L_M)/C_1}$. The current has the maximum at the time, $T/4 = p/2\sqrt{(L_1 + L_2 + L_M)C_1}$. Here, T is the period of the oscillation.

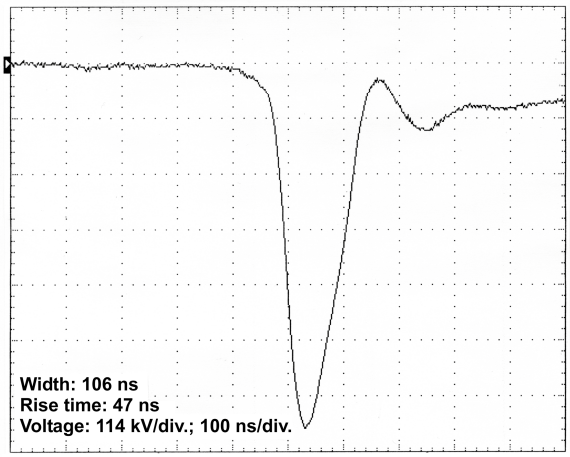

Figure 2. Voltage waveform measured across the exploding wire/fuse.

ELECTROMAGNETIC INDUCTION

If the diameter of the copper wire is decreased, the thin wire behaves as the exploding fuse. When the current through the fuse, I is interrupted at time interval ? t, the voltage, V_{fuse} is generated across the exploding wire. Reinovsky *et al.*[8] have derived the expression. Their formula can be interpreted as the sum of the current derivates:

$$V_{fuse} = \left[(L_1 + L_2 + L_M) \sum \frac{\Delta I}{\Delta t} \right] \exp\left(- \frac{R_W T^2}{2L} \right) \quad (1)$$

The time of interest, T starts around the quarter period when the voltage at the condensers in the Marx bank is at zero value. The fuse resistance, R_W was assumed to rise linearly with time, T up to the end of the "conduction time" of the fuse wire, t_c ($T = t - t_c$). By solving the circuit equation, Reinovsky *et al.* found that V_{fuse} takes the shape of the Gaussian function due to the term: $\exp(-\text{constant} \times T^2)$.

EXPERIMENTAL DATA

Fig. 2 is obtained when the wire of very small diameter is used. For example d = 0.04 mm. This wire/fuse explodes after the current through the wire has reached its

peak at about 300 ns. Keeping the switch U_2 open, the voltage at the output of the coil rises from 4.5 kV up to 750 kV. The latter value is similar to the data given by Fortov *et al.*[4] and Shimomura *et al.*[9]. Adding the corona ring at the output of the coil minimizes the unwanted glow-like discharges. In respect to the ground, this ring has the capacitance, C_2 (~ 100 pF).

When the switch U_2 is closed, Fig. 3 was obtained. After 300 ns, the current through the fuse starts to fall. The maximum slope, $?I/?t$ of the current interruption is 2.64×10^{10} A/s. For $L_1 + L_2 + L_M = 12.6$ μH, V_{fuse} is equal to 333 kV for this part of the waveform. To get the overall value for V_{fuse}, the current waveform is divided into segments and the current differential is obtained for each segment. Afterwards, Eq. 1 was used.

At first glance Eq. 1 underestimates V_{fuse}. By minimizing unwanted glow-like discharge, it is found that this leads to better agreement between the theory and experiments. If the coil of larger (>> 25 μH) inductance was used, the agreement is excellent.

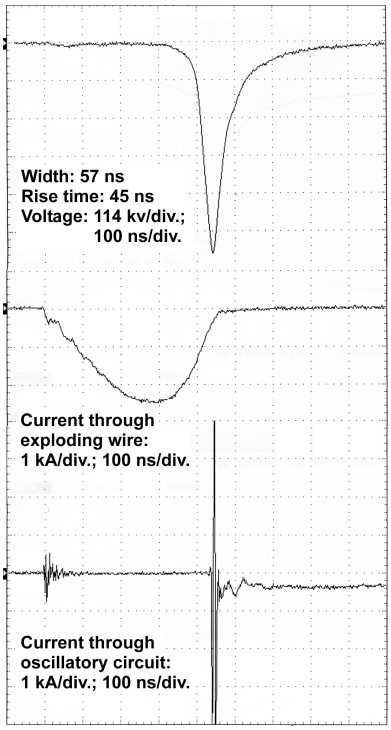

Figure 3. Currents and voltage waveforms after the switch U_2 is closed. The current through the fuse is recorded with the shunt using a low (550 MHz) pass filter.

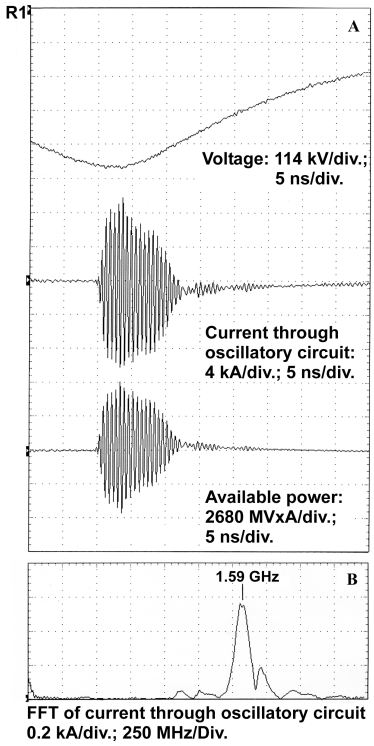

Figure 4. Frame A: Voltage and current waveforms. The zero reference for the voltage is marked by symbol R_1. Here, the voltage amplitude is 547 kV. The product of voltage and current is named the available power. Frame B: FFT of the current waveform.

In Figs. 3-5, the length of the wire was 30 cm and the applied voltage to Marx generator 24 kV/stage. In Figs. 6-9 the voltage was 26.2 kV/stage and the length of the wire was 24 cm.

Fig. 3 shows that the current through the oscillatory circuit has large spikes. The spikes exceed the scale used in this figure. To get the full amplitude, the current was recorded on the faster time (5 ns/div.) scale and the current (kA/div.) setting was increased. Data are given in Fig. 4.

RF emissions are given in Fig. 5. Before the wire/fuse explodes, the RF radiations are excited by the Marx generator and have strong 40 MHz and 170 MHz components. After the switch U_2 is closed, the emission commences at frequency of 1.59 GHz. The emissions were recorded by 10 GHz D-dot probe. This frequency is exactly the frequency of the current oscillations shown in Fig. 4. In most measurements after a few cycles, the emission is diverted to lower frequencies. In some measurements the frequency of 1.59 GHz and lower frequencies are initiated at the same time. For the first 30 ns, the relative distribution of RF emissions is given in Fig. 5, Frame B. The analysis of this data shows that most of its energy is emitted at low frequency of 40 MHz. By decreasing the length of the oscillatory circuit, the amount of emissions at higher frequencies can be enhanced at the expense of lower frequency emissions.

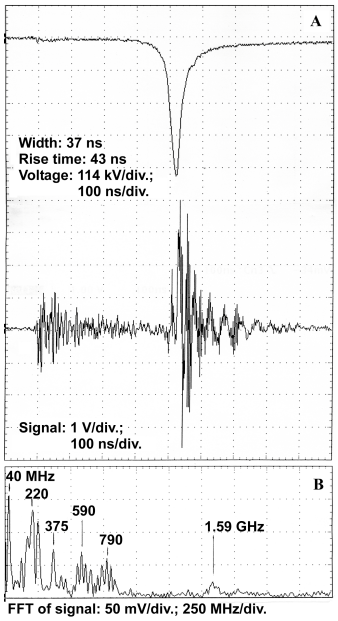

Figure 5. Frame A: Voltage and RF measurement using 10 GHz D-dot probe made by Prodyne Inc. The probe was placed at the distance of 1.25 m. The voltage amplitude is 479 kV in this shot. **Frame B:** FFT of the signal arising from the voltage impulse given at the top.

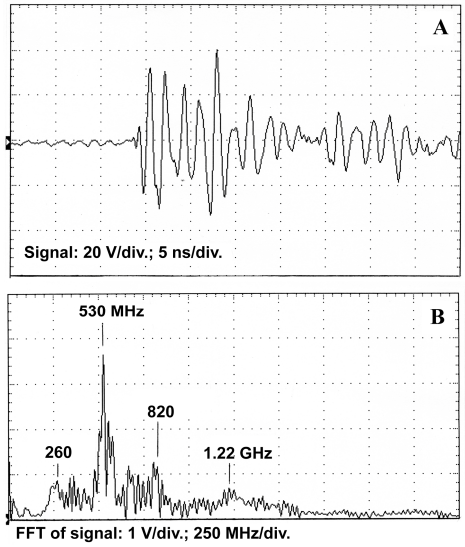

Figure 6. Frame A: RF pulse recorded by the single turn loop of 1.5 cm in diameter. The loop is placed 1.4 m away from the oscillatory circuit.

Frame B: FFT of the signal given in Frame A

The generation of RF radiations can be summarized in the following. When the wire explodes a high voltage impulse is created. The energy stored in the coil is compressed in time. This energy impulse charges C_2 of Fig. 1. The charged C_2 with the switch U_2 can be regarded as a "compact Marx" bank, which energizes the oscillatory circuit to create RF radiations.

Kekez[10] has postulated the mechanism of RF generations when the classical Marx generator is used to create RF radiations.

Fig. 8 gives the results "tuned" to radiate predominately at low frequency of 40 MHz by suppressing the radiations above this frequency. With a low 70 MHz filter, the maximum value of the electric field is 332 kV/m at frequency of 40 MHz and at distance of 1.25 m. By multiplying the signal by itself the relative shape of RF power was obtained. Power density is $E_2/(2Z_0)$ = 146 MW/m^2. Peak power is estimated to be 648 MW, the radiated energy over the width of 70 ns is 45 J, and the efficiency is the radiated energy of 45 J over $CV^2/2 \quad \left(=\left(7.5\times10^{-9}\right)\left(26.2\times10^{3}\right)^2/2 \ =92.6\ \mathrm{J}\right)$, which is 49%.

When the radiation is observed with the loop probe, Fig. 6 is obtained. We see that the induced voltage can reach the value of 40 V. Fig. 9 gives the emissions recorded by the BNC female connector. The FFT's of Figs. 8 and 9 can be related in part to the current waveform given in Fig. 10. All other conditions for this figure are as in Fig. 8.

To support this work, the generation of High Power Microwave (HPM) has also been investigated in some details. Powerful HPM signals of long duration are observed in the standing wave cavity in which a large-scale printed circuit board (of about 12" by 12") can be placed. The voltage recorded with the single turn loop of 1.89 cm in diameter exceeds 500 V when the frequency is 1.19 GHz. Work is currently under way on direct large (>1 MW) HPM generation.

CONCLUSION

With the use of an exploding wire as an opening switch, the energy stored in an inductor can be compressed in time to yield a high (up to 750 kV) voltage impulse with the available power of a few gigawatt range. A small (100 pF) capacitor, C_2 of Fig. 1 was added to the circuit to store the energy contained in the impulse. The charged C_2 is the part of the "compact Marx" generator. The oscillatory circuit consists of the closing (spark gaps) switches and a small line, represented by the symbol R in Fig. 1.

REFERENCES

1. Novac, B. *et al.*, "Fast numerical modelling and design issues of helical FCG's," *Proc. 14th IEEE International Pulsed Power Conference*, June 2003, pp. 417–420.
2. Freeman, B. *et al.*, "Similarity and differences between our small FCG's and large FCG's," *Proc. 14th IEEE International Pulsed Power Conference*, June 2003, pp. 409-412.
3. Chernychev, A., "Small helical explosive magnetic generators with magnetic flux capture," *Proc. 10th International Conference on Megagauss Field and Related Topics*, July 2004, pp. 90–94.

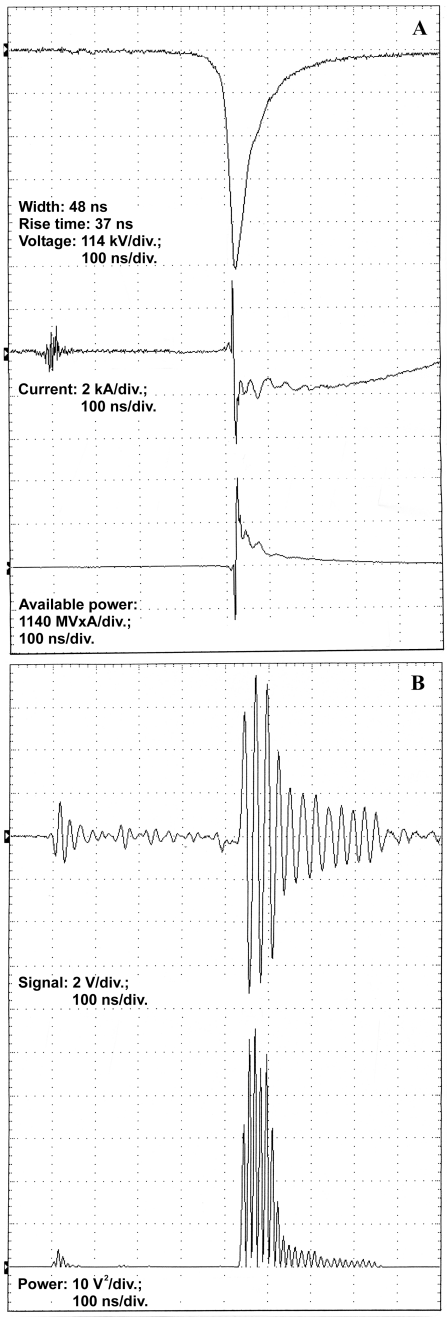

Figure 7. Frame A: Voltage, current and the product of voltage and current waveforms delivered to the oscillatory circuit. **Frame B:** RF signal recorded by D-dot probe with a low 70 MHz pass filter. The radiated power profile is obtained by multiplying the signal by itself.

4. Fortov, V. *et al.*, "Multipurpose generator for high power nanosecond H.V. pulses," *Proc. 9th International Conference on Megagauss Field and Related Topics*, July 2002, pp. 289–295.
5. Kristiansen, M. *et al.*, "Compact pulsed power and HPM devices," *The New World Vistas Programs*, Tech. Rep., 2003, report: AFRL-SR-TR-03-0463.
6. Selemir, V. *et al.*, "Conversion of MCG current pulse into H.V. pulse," *Proc. 9th International Conference on Megagauss Field and Related Topics*, July 2002, pp. 296-301.
7. Kekez, M.M., "Pulsed forming network-Marx pulsers for high power microwave applications," *Proc. 11th International Conference on High-Power Particle Beams*, June 1996.
8. Reinovksy, R. *et al.*, "High voltage power condition system powered by FCG's," *Proc. 7th IEEE Conference on Pulsed Power*, June 1989, pp. 971–974.
9. Shimomura, N. *et al.*, "Compact pulsed power generator using a Marx circuit and an exploding write," *Jpn. J. Applied Physics*, Vol. 40, Jan. 2001, pp. 4199–4204.
10. Kekez, M.M., "Contribution to radio frequency generation in regards to MCG," *Proc. 10th International Conference on Megagauss Field and Related Topics*, July 2004, pp. 135–143.

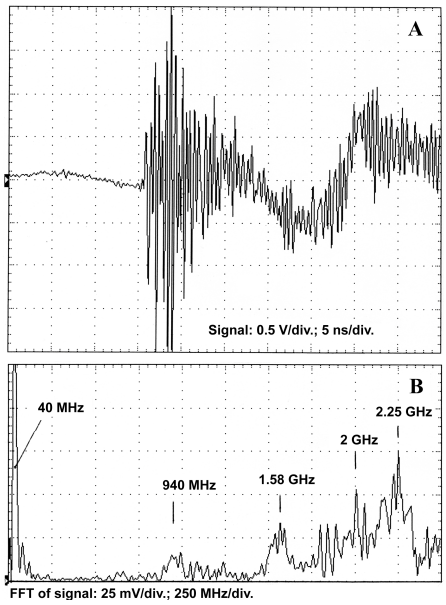

Figure 8. Frame A. Signal recorded by 50 O BNC female (Jack to jack) adapter. The adapter is placed 1.1 m away from the oscillatory circuit. **Frame B:** FFT of the signal given in Frame A.

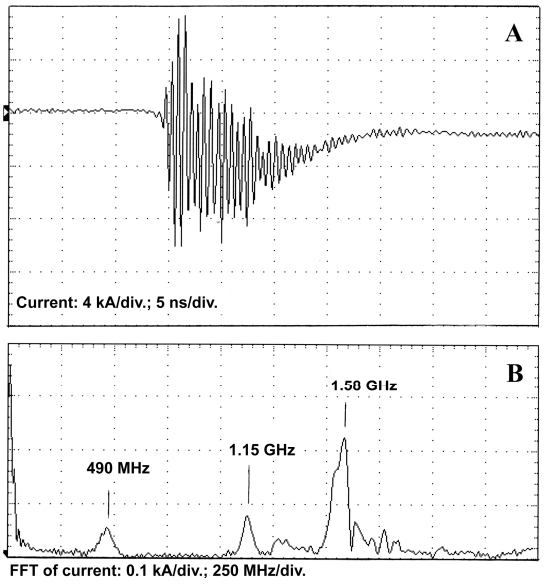

Figure 9. Frame A: Currents waveform after the switch U_2 is closed. **Frame B:** FFT of the signal given in Frame A. Figs. 6, 8, and 9 are synchronised in time.